JMEPEG (2005) 14:212-218
DOI: 10.1361/10599490523373

1059-9495/$19.00

# Tensile Properties of Martensitic Stainless Steels at Elevated Temperatures

*A.K. Roy, S.R Kukatla, B. Yarlagadda, V.N. Potluri, M. Lewis, M. Jones, and B.J. O'Toole*

*(Submitted November 2, 2004; in revised form January 18, 2005)*

**Tensile properties of quenched and tempered martensitic alloys EP-823, HT-9, and 422 were evaluated at temperatures ranging from ambient to 600 °C as a function of three different tempering times. The results indicated that the yield strength, ultimate tensile strength, and the failure strength were gradually reduced with increasing temperature. The ductility parameters were enhanced at elevated temperatures due to increased plastic flow. However, the tempering time did not significantly influence these properties. The evaluation of the fracture surfaces by scanning electron microscopy revealed reduced cracking and dimpled microstructures, indicating enhanced ductility at higher testing temperatures.**

**Keywords** elevated temperatures, martensitic alloys, scanning electron microscopy, tensile properties

## 1. Introduction

The disposal of nuclear waste poses a severe challenge to all nuclear power-generating nations. Significant efforts are ongoing to dispose of high-level radioactive waste (HLW) and spent nuclear fuel (SNF) in a geologic repository located at the Yucca Mountain site near Las Vegas, Nevada. Because these HLWs and SNFs have long half-lives, they will need to be stored for an unusually long time inside the proposed repository. In view of this rationale, significant attention is currently being focused on reducing the half-life and radioactivity of these nuclear fuels by a process known as transmutation. This process involves bombarding a target material such as the molten lead-bismuth-eutectic (LBE) using protons generated by an accelerator or a reactor, thereby producing neutrons. These neutrons are then impinged upon the HLW and SNF at a very high speed, thus transforming long-lived isotopes into species with relatively short half-lives and reduced radioactivity through the capture and decay of minor actinides and fission products. This reduction in half-life and radioactivity may enable the disposal of HLW and SNF for shorter durations in the proposed repository.

During the transmutation process, a significant amount of heat can be generated in the molten LBE target material, which will be contained in a subsystem structural container made of a suitable martensitic iron-chromium-molybdenum (Fe-Cr-Mo) stainless steels, such as EP-823, HT-9, and 422. The selection of these materials is based on their excellent resistance to void swelling under irradiation, irradiation creep properties, and low coefficient of thermal expansion (Ref 1, 2). These materials will be subjected to high tensile stresses while they are in contact with the LBE at temperatures ranging between 400 and 600 °C. Therefore, a research program was initiated to evaluate the deformation characteristics of all three alloys in properly heat-treated conditions at temperatures relevant to the operating environment. This article presents the results of tensile testing of all three materials at temperatures ranging from ambient to 600 °C in the presence of nitrogen. The results of metallographic and fractographic evaluations are also presented.

**A.K. Roy, S.R Kukatla, B. Yarlagadda, V.N. Potluri, M. Lewis, M. Jones,** and **B.J. O'Toole,** Department of Mechanical Engineering, University of Nevada Las Vegas, 4505 Maryland Parkway, Box 454027, Las Vegas, NV 89154. Contact e-mail: aroy@unlv.nevada.edu.

## 2. Experimental

Experimental heats of EP-823, HT-9, and 422 stainless steels were vacuum-induction-melted, then forged and hot rolled. Subsequently, the hot-rolled bars were thermally treated to produce a fully tempered and fine-grained martensitic microstructure without any retained austenite. They were austenitized at 1850 °F, oil-quenched, and tempered at 1150 °F, then underwent air-cooling. The tempering operation was performed on the EP-823, HT-9, and 422 stainless steels for 1.25, 1.75, and 2.25 h, respectively, to study the effect of tempering time on the tensile properties. The hardness of all materials, before and after tempering, was measured using the Rockwell hardness scale. The chemical compositions of all three materials are given in Table 1. Compared to the other two martensitic stainless steels, EP-823 had a lower C content, but a higher Si content. This is a Russian-grade alloy that was specifically designed for nuclear applications. All three alloys contained Ni, V, and W.

Smooth cylindrical specimens, 100 mm in length, and with a 25 mm gage length and 6.35 mm gage diameter, were machined from the heat-treated round bars in such a way that the gage section was parallel to the longitudinal rolling direction. The tensile properties were determined at temperatures ranging from ambient to 600 °C by using a computer-controlled mechanical testing system according to ASTM standard E 8 (Ref 3). The specimens were loaded in tension at a strain rate of $10^{-3}$ $s^{-1}$. A minimum of two specimens was tested under each condition, with the average value recorded. All elevated temperature tests were performed in the presence of nitrogen injected inside a ceramic heating chamber to prevent contamination from the surrounding atmosphere.

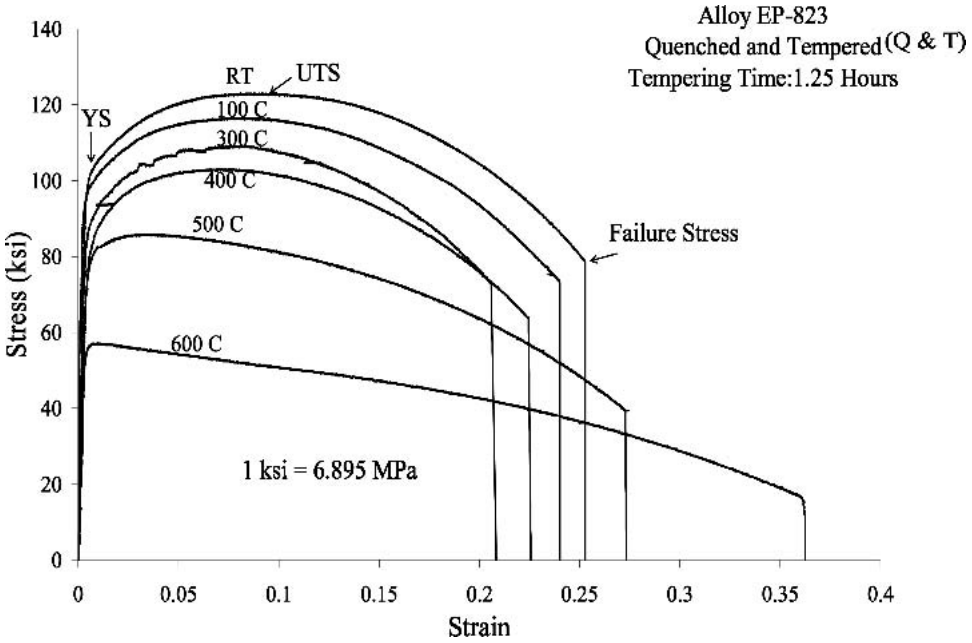


**Fig. 1** Comparison of s-e diagrams for alloy EP-823 at different test temperatures

**Table 1 Chemical compositions of materials tested, (wt.%)**

| Material/heat number | C | Mn | P | S | Si | Cr | Ni | Mo | Cu | V | W | Cb | B | Ce |
|---|---|---|---|---|---|---|---|---|---|---|---|---|---|---|
| HT-9/2049 | 0.19 | 0.41 | 0.012 | 0.004 | 0.20 | 12.31 | 0.50 | 1.00 | 0.01 | 0.30 | 0.47 | … | … | … |
| EP-823/2056 | 0.14 | 0.56 | 0.013 | 0.005 | 1.11 | 11.68 | 0.66 | 0.73 | 0.002 | 0.30 | 0.62 | 0.22 | 0.009 | 0.05 |
| 422/2053 | 0.20 | 0.54 | 0.012 | 0.004 | 0.49 | 12.76 | 0.74 | 0.97 | 0.002 | 0.22 | 0.92 | … | … | … |

The metallurgical microstructures of the tested specimens were evaluated by optical microscopy. The primary fracture surface of the tensile specimens was analyzed by scanning electron microscopy (SEM) to determine the extent and morphology of failure.

## 3. Results and Discussion

The hardness ($R_c$) values of the three alloys for the different heat-treatment conditions are given in Table 2. A gradual decrease in $R_c$ values was obtained with increases in tempering time. This reduction in $R_c$ values with longer tempering time may be attributed to the homogenization of the metallurgical microstructure and the minimization or elimination of internal stresses resulting from the quenching operation following the austenitization of the test materials.

Comparisons of the engineering stress-strain (s-e) diagrams at different testing temperatures using specimens quenched and tempered for 1.25 h are illustrated in Fig. 1 to 3 for EP-823, HT-9, and 422 stainless steels, respectively. An examination of these figures clearly indicates that the magnitude of the yield strength (YS), ultimate tensile strength (UTS), and failure stress ($\sigma_f$) gradually decreased with increasing testing temperature. A similar trend was also observed with specimens quenched and tempered for longer durations (i.e., 1.75 and 2.25 h). It is interesting to note that the reduction in strength was more pronounced at temperatures above 400 °C, suggesting that a critical temperature may exist for these martensitic stainless steels above which the plastic flow can be significantly enhanced due to the faster movement of lattice imperfections

**Table 2 Hardness values versus thermal treatment**

| | $R_c$ | | |
|---|---|---|---|
| **Heat treatment** | **EP-823** | **422** | **HT-9** |
| Austenitized 1010 °C/1 h/OQ | 39 | 48 | 52 |
| Q&T at 620 °C/1.25 h/AC | 28 | 32 | 31 |
| Q&T at 620 °C/1.75 h/AC | 26 | 28 | 28 |
| Q&T at 620 °C/2.25 h/AC | 24 | 27 | 27 |

Note: Q&T, quenched and tempered; OQ, oil-quenched; AC, air-cooled

such as dislocations and voids through their grain boundaries. This type of thermally activated dislocation motion in martensitic alloys is consistent with observations made by other investigators (Ref 4-6). Another observation of note in the samples tested above 400 °C is that the uniform elongation was reduced to the point where the UTS became almost equal to the YS.

An evaluation of the s-e diagrams, shown in Fig. 1 to 3, also reveals that the strain gradually decreased with increasing temperature in the temperature regimen of ambient to 300 °C. This was followed by increased strains at temperatures beyond 300 °C. Such phenomenon may be attributed to dynamic strain hardening resulting from locking of dislocations in the vicinity of grain boundaries at relatively lower temperatures, thus reducing plastic flow. Similar behavior has been reported for other martensitic alloys (Ref 4-6).

The effect of temperature on YS, UTS, percent elongation (%El), and percent reduction in area (%RA) for EP-823, HT-9, and 422 stainless steels is shown in Tables 3 to 5, respectively,

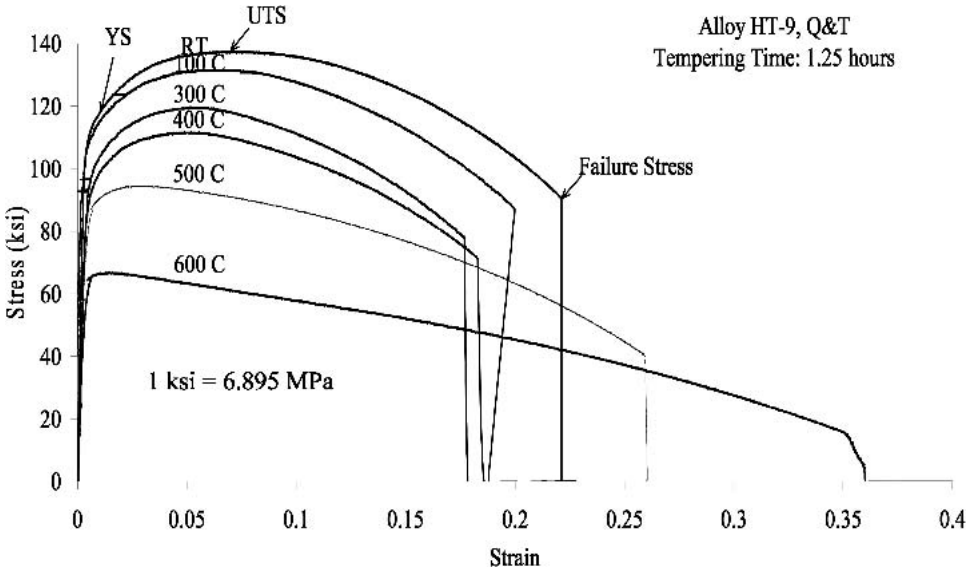


**Fig. 2** Comparison of s-e diagrams for alloy HT-9 at different test temperatures

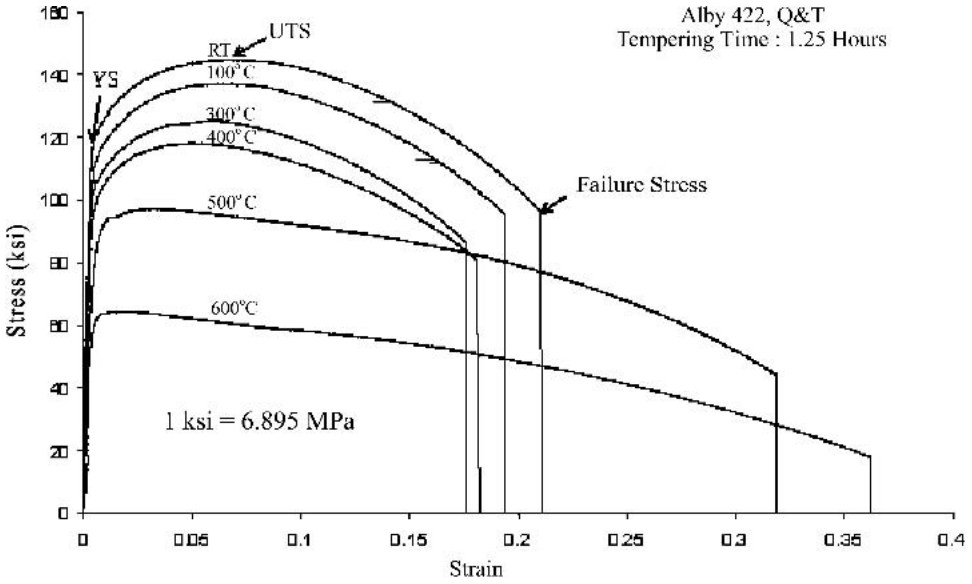


**Fig. 3** Comparison of s-e diagrams for alloy 422 at different temperatures

as a function of the tempering time. These data reveal that with increasing temperature the magnitude of YS and UTS decreased, as indicated earlier. Simultaneously, the ductility in terms of %El was lower at temperatures between ambient and 300 °C due to dynamic strain aging followed by a gradual increase at temperatures beyond 300 °C. However, no significant effect of tempering time on these parameters was observed with any of these alloys, possibly due to the fact that the tempering times were too close together and of short duration.

The data presented in Tables 3 through 5 are reproduced in Fig. 4 to 7. These figures show the effect of temperature on YS, UTS, %El, and %RA for all three alloys quenched and tempered for 1.25 h. Once again, a gradual reduction in YS and UTS with increasing temperature is illustrated in Fig. 4 and 5, respectively. The relatively lower YS and UTS (and $R_c$ values shown in Table 2) of EP-823 stainless steel under ambient conditions may be attributed to its relatively lower C content and thus, the reduced density of carbides ($M_{23}C_6$ type) compared with that in HT-9 and 422 stainless steels. It is also interesting to note that both the YS and UTS of 422 stainless steel under ambient conditions were somewhat higher than those of HT-9 stainless steel. The higher strength of 422 stainless steel may be due to the presence of a higher Cr + Ni content (13.15 versus 12.81), thus enhancing solid-solution strengthening (Ref 7).

A comparison of ductility in terms of %El (shown in Fig. 6) revealed a slight decrease because the temperature increased from ambient to 300 °C, followed by a gradual increase as the temperature increased from 300 °C. With respect to %RA, an insignificant variation was observed in the temperature range of ambient to 300 °C, once again followed by a gradual increase with increasing temperature (shown in Fig. 7). Thus, the

**Table 3 Tensile properties of EP-823 as a function of temperature**

| Tensile properties | Tempering time, h | Testing temperature, °C | | | | | |
|---|---|---|---|---|---|---|---|
| | | Ambient | 100 | 300 | 400 | 500 | 600 |
| YS, ksi | 1.25 | 102 | 97 | 89 | 87 | 77 | 57 |
| (MPa) | | (702) | (668) | (613) | (599) | (533) | (394) |
| | 1.75 | 103 | 97 | 89 | 84 | 78 | 57 |
| | | (713) | (671) | (614) | (581) | (535) | (394) |
| | 2.25 | 101 | 96 | 90 | 81 | 75 | 56 |
| | | (700) | (661) | (619) | (562) | (516) | (383) |
| UTS, ksi | 1.25 | 125 | 117 | 110 | 105 | 85 | 59 |
| (MPa) | | (860) | (808) | (760) | (727) | (585) | (407) |
| | 1.75 | 124 | 116 | 109 | 103 | 84 | 59 |
| | | (858) | (803) | (753) | (710) | (580) | (405) |
| | 2.25 | 124 | 116 | 110 | 102 | 84 | 56 |
| | | (853) | (797) | (761) | (703) | (576) | (389) |
| %E1 | 1.25 | 24.8 | 23.7 | 20.4 | 22.4 | 30.0 | 36.5 |
| | 1.75 | 24.4 | 23.3 | 21.6 | 21.8 | 28.4 | 38.3 |
| | 2.25 | 24.3 | 22.9 | 21.1 | 21.7 | 29.9 | 41.8 |
| %RA | 1.25 | 63.8 | 64.6 | 63.6 | 65.4 | 75.3 | 85.0 |
| | 1.75 | 65.0 | 65.4 | 64.1 | 65.3 | 76.8 | 85.7 |
| | 2.25 | 64.1 | 66.4 | 64.6 | 66.5 | 77.5 | 86.2 |

**Table 4 Tensile properties of HT-9 as a function of temperature**

| Tensile properties | Tempering time, h | Testing temperature, °C | | | | | |
|---|---|---|---|---|---|---|---|
| | | Ambient | 100 | 300 | 400 | 500 | 600 |
| YS, ksi | 1.25 | 111 | 102 | 98 | 92 | 87 | 65 |
| (MPa) | | (768) | (705) | (675) | (632) | (601) | (448) |
| | 1.75 | 111 | 102 | 95 | 90 | 85 | 63 |
| | | (767) | (700) | (656) | (623) | (587) | (436) |
| | 2.25 | 110 | 101 | 94 | 89 | 85 | 62 |
| | | (762) | (700) | (650) | (614) | (584) | (429) |
| UTS, ksi | 1.25 | 138 | 133 | 119 | 112 | 95 | 66 |
| (MPa) | | (955) | (914) | (820) | (772) | (654) | (458) |
| | 1.75 | 137 | 127 | 115 | 110 | 92 | 65 |
| | | (947) | (878) | (795) | (757) | (635) | (446) |
| | 2.25 | 135 | 125 | 114 | 107 | 91 | 64 |
| | | (931) | (865) | (788) | (740) | (629) | (440) |
| %El | 1.25 | 21.1 | 19.3 | 17.4 | 18.5 | 26.9 | 35.8 |
| | 1.75 | 19.6 | 20.6 | 17.6 | 18.4 | 26.4 | 36.1 |
| | 2.25 | 20.5 | 19.9 | 17.8 | 18.1 | 25.8 | 37.4 |
| %RA | 1.25 | 58.5 | 62.2 | 62.5 | 63.3 | 77.6 | 87.5 |
| | 1.75 | 58.7 | 62.3 | 63.1 | 641 | 78.4 | 88.4 |
| | 2.25 | 58.5 | 62.8 | 62.1 | 64.3 | 78.5 | 88.8 |

**Table 5 Tensile properties of 422 as a function of temperature**

| Tensile properties | Tempering time, h | Testing temperature, °C | | | | | |
|---|---|---|---|---|---|---|---|
| | | Ambient | 100 | 300 | 400 | 500 | 600 |
| YS, ksi | 1.25 | 119 | 113 | 103 | 91 | 87 | 62 |
| (MPa) | | (820) | (783) | (710) | (627) | (600) | (430) |
| | 1.75 | 119 | 115 | 104 | 91 | 87 | 62 |
| | | (820) | (794) | (716) | (631) | (601) | (426) |
| | 2.25 | 116 | 112 | 102 | 97 | 88 | 64 |
| | | (802) | (770) | (701) | (667) | (609) | (441) |
| UTS, ksi | 1.25 | 144 | 137 | 126 | 118 | 98 | 65 |
| (MPa) | | (996) | (945) | (869) | (817) | (673) | (451) |
| | 1.75 | 145 | 137 | 126 | 116 | 97 | 66 |
| | | (1003) | (942) | (867) | (803) | (667) | (454) |
| | 2.25 | 142 | 135 | 125 | 119 | 98 | 66 |
| | | (982) | (930) | (864) | (818) | (675) | (458) |
| %El | 1.25 | 21.1 | 19.7 | 17.6 | 18.5 | 37.6 | 45.5 |
| | 1.75 | 21.0 | 20.3 | 17.6 | 18.4 | 31.5 | 47.5 |
| | 2.25 | 21.0 | 19.7 | 18.0 | 18.6 | 26.7 | 39.5 |
| %RA | 1.25 | 58.6 | 60.3 | 61.3 | 63.2 | 74.3 | 88.8 |
| | 1.75 | 58.6 | 61.8 | 62.1 | 64.8 | 75.5 | 89.4 |
| | 2.25 | 60.8 | 61.2 | 61.8 | 64.1 | 76.9 | 89.3 |

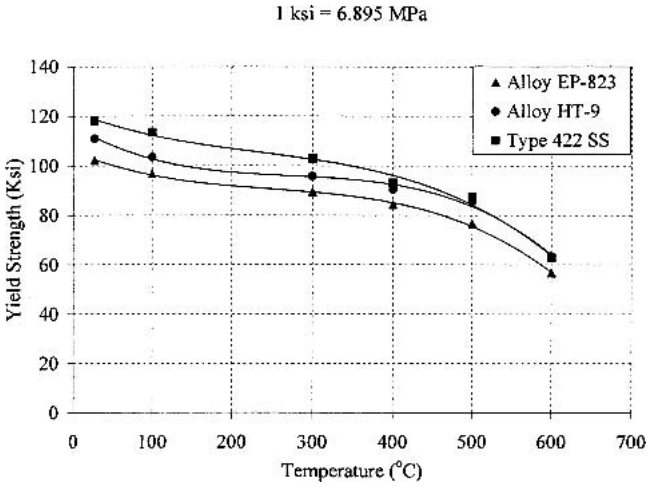


**Fig. 4** Average YS as a function of temperature

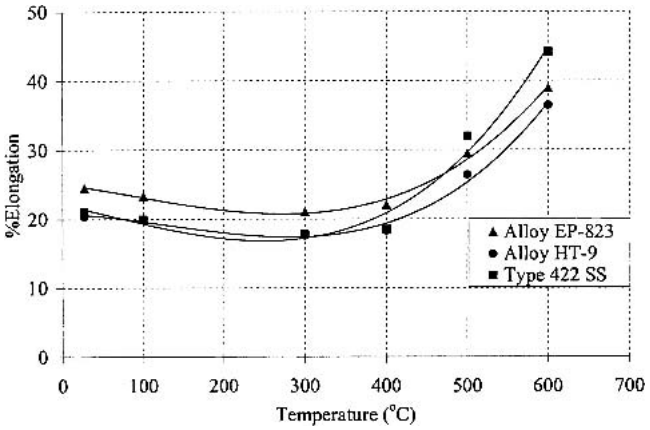


**Fig. 6** Average %El as a function of temperature

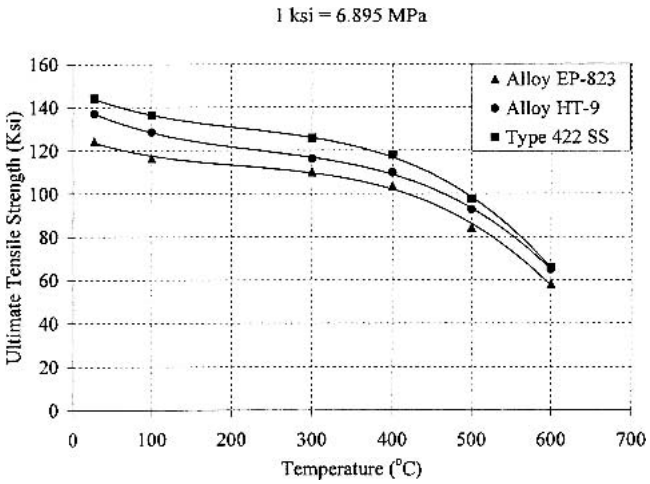


**Fig. 5** Average UTS as a function of temperature

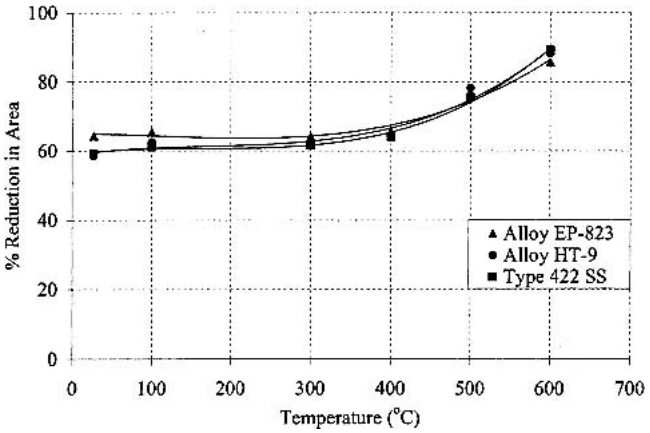


**Fig. 7** Average %RA in area as a function of temperature

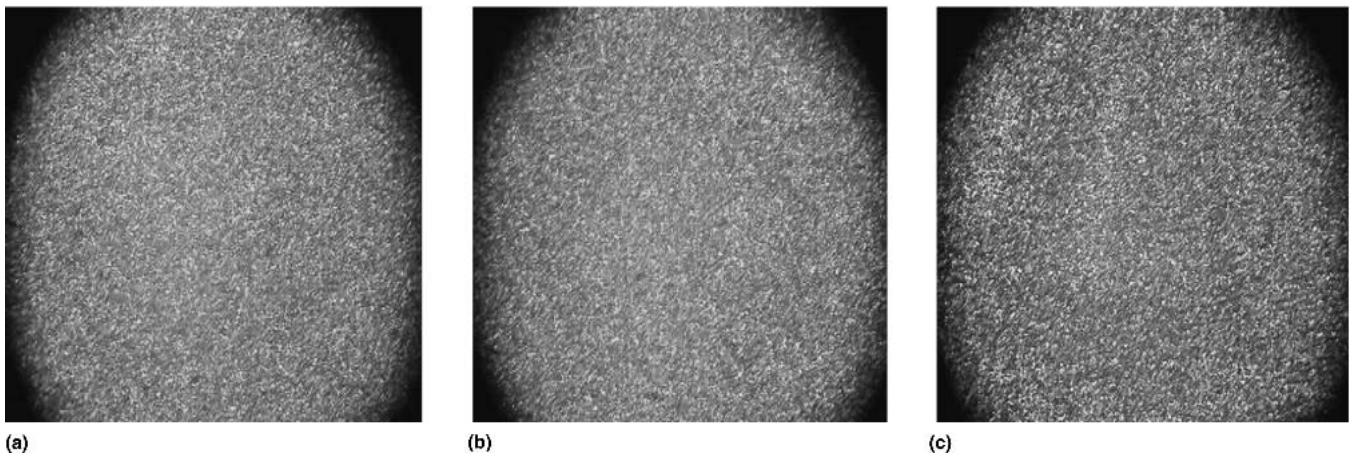


**Fig. 8** Optical micrographs of quenched and tempered EP-823 stainless steel as a function of tempering (with Fry's reagent-5X) time: (a) 1.25 h; (b) 1.75 h; and (c) 2.25 h

overall tensile data appear to be consistent with results cited in the open literature for similar types of alloys (Ref 4-6).

The optical micrographs of the EP-823 stainless steel, quenched and tempered for 1.25, 1.75, and 2.25 h, are illustrated in Fig. 8, and show a fine-grained, tempered, martensitic microstructure. It is interesting to note that the difference in tempering time did not influence the resultant microstructure of EP-823 stainless steel, possibly due to the narrow range of

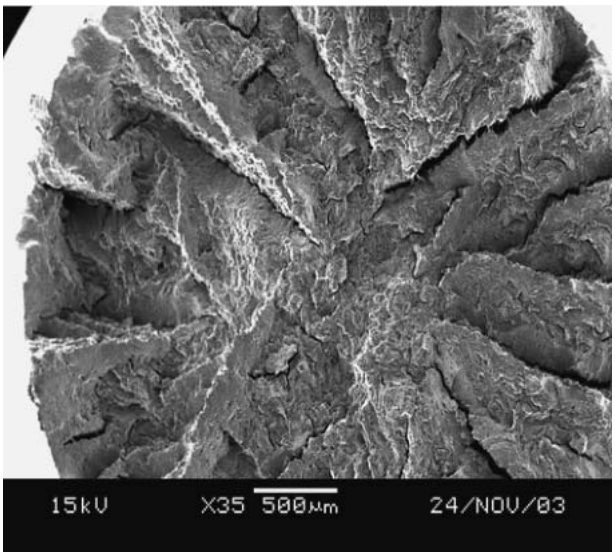


**Fig. 9** SEM micrograph of alloy HT-9 at room temperature (magnification 35×)

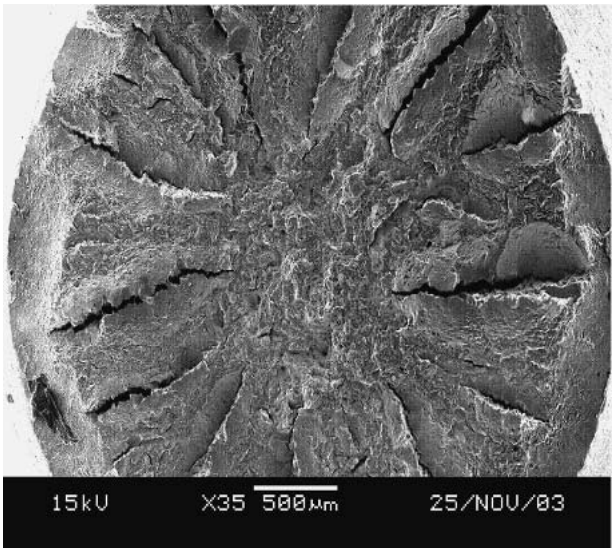


**Fig. 10** SEM micrograph of alloy HT-9 at 100 °C (magnification 35×)

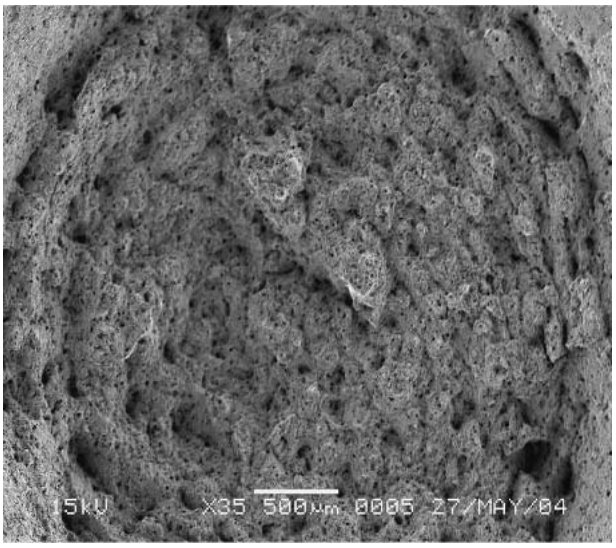


**Fig. 11** SEM micrograph of alloy HT-9 at 300 °C (magnification 35×)

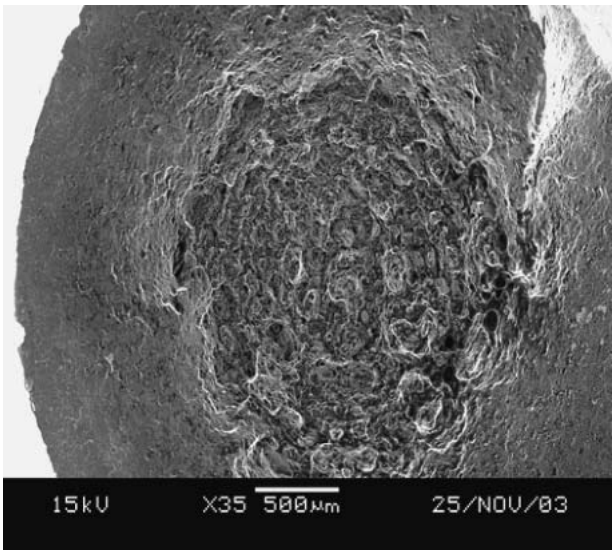


**Fig. 12** SEM micrograph of alloy HT9 at 600 °C (magnification 35×)

tempering times. Similar microstructural characteristics were observed with HT-9 and 422 stainless steels. The results of the SEM study of the primary fracture surface of the HT-9 stainless steel at different temperatures are illustrated in Fig. 9 to 12. An examination of these micrographs revealed a large number of cracks with little or no plasticity that developed at room temperature and 100 °C. However, plasticity, characterized by reduced cracking and dimpled microstructures, was observed at higher test temperatures, indicating improved ductility. Once again, the tempering time did not influence the mode of failure in any tested materials.

## 4. Summary and Conclusions

The tensile properties of martensitic stainless steels EP-823, HT-9, and 422 were evaluated at ambient and elevated temperatures in the presence of nitrogen. Metallographic and fractographic evaluations of the alloys were performed using optical microscopy and SEM. The significant conclusions derived from this investigation are summarized below.

- The $R_c$ values of all three austenitized and quenched alloys decreased with tempering time.
- The magnitude of YS, UTS, and $\sigma_f$ decreased with increasing temperature, and showed significant decreases at temperatures above 400 °C.
- The extent of ductility in terms of %El decreased to a minimum in the temperature range of ambient to 300 °C due to dynamic strain hardening. Beyond 300 °C, the %El gradually increased due to increased plastic flow.
- The morphology of failure was characterized by increased plastic deformation at elevated temperatures. Reduced cracking and dimpled microstructures were observed on the fracture surfaces.
- The tempering time did not influence the microstructure and the resultant tensile properties to any great extent, possibly due to the short and narrow range in tempering time.

## Acknowledgment

This work was funded through the University of Nevada, Las Vegas, Transmutation Research Program, and was administered by the Harry Reid Center for Environmental Studies (U.S. Department of Energy grant No. DE-FG04-2001 AL67358).

## References

1. D.R. Harries, The Materials Requirements for NET, *Radiat. Eff. Defects Solids,* Vol 161, 1987, p 3
2. R.L. Klueh, K. Ehrlich, and F. Abe, *Ferritic/Martensitic Steels: Promises and Problems, J. Nucl. Mater.,* Vol 116, 1992, p 191-194
3. "Standard Test Methods for Tension Testing of Metallic Materials," E 8-01, *Annual Book of ASTM Standards,* ASTM, 2001
4. D. Gavillet, P. Marmy, and M. Victoria, The Microstructure of the 1.4914 MANET Martensitic Steel before and after Irradiation with 590 MeV Protons, *J. Nucl. Mater.,* Vol 890, 1992, p 191-194
5. P. Marmy, J.L. Martin, and M. Victoria, Deformation Mechanisms of Ferritic–Martensitic Steel Between 290 and 870 K, *Mater. Sci. Eng.,* Vol A164, 1993, p 159-163
6. M. Victoria, D. Gavillet, P. Spatig, F. Rezai-Aria, and S. Rossmann, Microstructure and Mechanical Properties of Newly Developed Low Activation Martensitic Steels, *J. Nucl. Mater.,* Vol 233-237, 1996, p 326-330
7. S. Floreen, The Properties of Low Carbon Iron-Nickel-Chromium Martensites, *Trans. Am. Inst. Min. Metall. Pet. Eng.,* Vol 236, 1966, p 1429-1440